# Polarization-sensitive optical coherence tomography for the nondestructive assessment of the remineralization of dentin

**Saman K. Manesh**
**Cynthia L. Darling**
**Daniel Fried**
University of California
Department of Preventative and Restorative Dental Sciences
San Francisco, California 94143-0758

**Abstract.** Previous studies have demonstrated that polarization-sensitive optical coherence tomography (PS-OCT) can be used to image caries lesions in dentin, measure nondestructively the severity of dentin demineralization, and determine the efficacy of intervention with anticaries agents including fluoride and lasers. The objective of this study is to determine if PS-OCT can be used to nondestructively measure a reduction in the reflectivity of dentin lesions after exposure to a remineralization solution. Although studies have shown the ability of PS-OCT to image the remineralization of lesions in enamel, none have included dentin. PS-OCT images of dentin surfaces are acquired after exposure to an artificial demineralizing solution for six days and a remineralizing solution for 20 days. The integrated reflectivity, depth of demineralization, and thickness of the layer of remineralization are calculated for each of the two treatment groups on each sample. Polarized light microscopy and microradiography are used to measure lesion severity on histological thin sections for comparison. PS-OCT successfully measured the formation of a layer of increased mineral content near the lesion surface. Polorized light microscopy (PLM) and transverse microradiography (TMR) corroborated those results. PS-OCT can be used for the nondestructive measurement of the remineralization of dentin.  [DOI: 10.1117/1.3158995]

Keywords: polarization-sensitive optical coherence tomography; dentin; demineralization; remineralization artificial lesions; caries inhibition topical fluoride.

Paper 09061PR received Feb. 23, 2009; revised manuscript received May 4, 2009; accepted for publication May 11, 2009; published online Jul. 1, 2009. This paper is a revision of a paper presented at the SPIE conference on Lasers in Dentistry XV, January 2009, San Jose, California. The paper presented there appears (unrefereed) in SPIE Proceedings Vol. 7162.

## 1 Introduction

Several studies over the past few years have demonstrated that optical coherence tomography (OCT) can be used for the assessment of the severity of early caries lesions. OCT is a noninvasive technique for creating cross sectional images of internal biological structure.[1–3] It is nondestructive and has great potential for imaging *in vivo*. Polarization-sensitive OCT (PS-OCT) is a form of OCT that is sensitive to changes in the polarization of the reflected light.[4] PS-OCT, has been successfully used to acquire images of both artificial and natural caries lesions, assess their severity in depth, assess the remineralization of such lesions on enamel,[3–5] and determine the efficacy of chemical agents in inhibiting demineralization.[5] Recent studies in our laboratory on dentin and cementum surfaces demonstrate that PS-OCT is also well suited to assess the severity of demineralization on those surfaces, as well as determine the efficacy of anticaries agents such as fluoride and lasers.[6,7]

One of the most promising applications of PS-OCT is the nondestructive measurement of the remineralization of existing caries lesions. *In-vitro* measurements of the remineralization of artificial lesions produced on enamel surfaces demonstrated that the thickness of the thin layer of higher mineral content that is typically formed near the lesion surface during the remineralization process can be measured with PS-OCT.[8–10] This layer is of considerable importance, since the formation of this layer of fluoroapatite limits diffusion into the lesion leading to the arrest of lesion progression, and the lesion becomes inactive and there is no further need for intervention.

Polarization-sensitive depth-resolved reflectivity measurements can provide a measure of the severity of natural and artificial caries lesions on smooth surfaces and in occlusal pits and fissures.[11–14] The high reflectivity of dentin and enamel

Address all correspondence to Daniel Fried, PhD, Professor, Director, MS Program in Oral & Craniofacial Biology, Division Biomaterials and Bioengineering, Department of Preventive and Restorative Dental Sciences, University of California, San Francisco, 707 Paranassus Ave., San Francisco, CA 94143-0758. Tel: 415-502-6641; Fax: 415-476-0858; E-mail: daniel.fried@ucsf.edu

1083-3668/2009/14(4)/044002/6/$25.00 © 2009 SPIE

surfaces produces a very strong reflection that can interfere with the measurement of early demineralization on the surface. This strong reflection can be reduced using polarized light. Moreover, demineralized areas on the tooth depolarize the incident linearly polarized light, and the reflectivity in the orthogonal or perpendicular polarization state to the incident polarization can be directly integrated to provide a measure of the lesion severity.

Although the penetration depth of near-IR light is considerably less in dentin than for enamel due to the markedly higher scattering coefficient of dentin, PS-OCT and OCT images of dentin with root caries show that penetration depths of ~1 mm can be achieved, demineralized dentin can be discriminated from sound dentin and cementum,[15] and root canal walls and fractures can be imaged.[16,17] In contrast to sound enamel that is highly transparent in the near-IR, sound dentin strongly scatters light in the near-IR and is highly birefringent.[18,19] Even with this limitation, we have successfully demonstrated that a similar approach to that used to assess the severity of demineralization on enamel surfaces can be applied to the dentin surfaces as well.[6,7] Amaechi et al.[20] measured the percent reflectivity loss due to demineralization on dentin surfaces, and showed that this correlated well with mineral loss from microradiography. However, the validity of an approach that relies on the measurement of reflectivity loss is questionable, since light scattering increases with demineralization for both enamel and dentin, producing an overall increase in reflectivity from the area of the lesion, not a decrease in reflectivity. The approach that we have chosen is to measure the reflectivity from each layer of the lesion and subsequently integrate over a specific depth to yield the integrated reflectivity ($\Delta R$) in units of dB $\times$ $\mu$m, which is compared with the "gold standard"—the integrated mineral loss ($\Delta Z$) that is calculated in a similar fashion by integrating the mineral loss over a specific depth.[11–14,21]

It has been well established that topical fluoride agents can inhibit the demineralization of enamel, dentin, and cementum.[22] Current methods that are used to determine the efficacy of anticaries agents require teeth scheduled for extraction and partial destruction of the tooth through sectioning. These methods include microradiography, microhardness, and polarized light microscopy.

In summary, the principal objective of this study was to demonstrate that a significant reduction in the reflectivity from the area of dentin lesions can be measured using PS-OCT after exposure of those lesions to a remineralization solution. PS-OCT measurements were also compared with the well established methods of transverse microradiography and polarized light microscopy that require tooth extraction and thin sectioning.

## 2 Materials and Methods

### 2.1 *Sample Preparation*

15 dentin blocks, approximately $6 \times 3 \times 2$ mm$^3$, were prepared from extracted human teeth for this study. The dentin surfaces were serial polished to one micron using embedded diamond polishing disks. Two windows on each sample were exposed to the demineralization solution, and one window was exposed to the remineralization solution (Fig. 1). The middle partition of each sample and both ends was covered

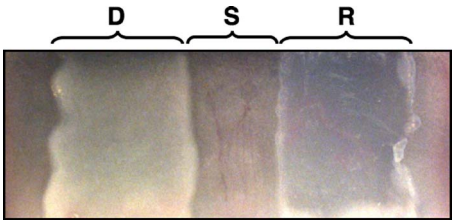


**Fig. 1** Reflected light image of a representative tooth sample after demineralization and remineralization showing the three study groups D, S, and R. The remineralized layer is clearly visible on the (R) group as compared to its (D) group counterpart.

with a thin layer of acid-resistant varnish red nail polish (Revlon, New York) to protect the sound dentin control area before exposure to the demineralization solution. Samples were placed in a demineralization solution for six days with both windows exposed consisting of a 40-mL aliquot of 2.0-mmol/L calcium, 2.0-mmol/L phosphate, and 0.075 mol/L acetate at pH 4.9, kept at a constant temperature of 37 °C. One window was covered with acid-resistant varnish, leaving the other window exposed. The samples were placed in a solution for remineralization consisting of 1.5-mmol/L calcium, 0.9-mmol/L phosphate, 150-mmol/L KCl, and 20-mmol/L cacodylate buffer maintained at pH 7.0 and 37 °C for 20 days. Fluoride, as NaF, was added at the level of 2-ppm F to enhance remineralization.[23]

### 2.2 *Polarization Sensitive Optical Coherence Tomography System*

A single-mode fiber autocorrelator-based optical coherence domain reflectometry (OCDR) system with polarization switching probe, high efficiency piezoelectric fiber stretchers, and two balanced InGaAs receivers that was designed and fabricated by Optiphase, Incorporated (Van Nuys, California) was integrated with a broadband high power superluminescent diode (SLD) (Denselight, Jessup, Maryland), with an output power of 45 mW, a bandwidth of 35 nm, and a high-speed *xy*-scanning system, ESP 300 controller, and 850-HS stages (Newport, Irvine, California), and used for *in-vitro* optical tomography. The system was configured to provide axial resolution at 22 $\mu$m in air and 16 $\mu$m in dentin, and a lateral resolution of approximately 50 $\mu$m over the depth of focus of 10 mm. The all-fiber OCDR system is described in more detail in Ref. 24 The PS-OCT system was completely controlled using LabVIEW™ software (National Instruments, Austin Texas).

### 2.3 *Polarized Light Microscopy and Transverse Microradiography*

After the dentin samples were imaged with PS-OCT, they were cut into sections approximately 200 to 260 $\mu$m thick using an Isomet 5000 saw (Buehler, Lake Bluff, Illinois) for polarized light microscopy (PLM) and digital transverse microradiography (TMR). PLM was carried out using a Meiji Techno RZT microscope (Meiji Techno Company, Limited, Saitama, Japan) with an integrated digital camera EOS Digital Rebel XT (Canon Incorporated, Tokyo, Japan). The sample sections were imbibed in water and examined in the bright-field mode with crossed polarizers and a red I plate with

500-nm retardation. A custom-built digital transverse microradiography (TMR) system was used to measure mineral loss in the different partitions of the sample.[25]

### 2.4 *Integrated Reflectivity, Quantitative Mineral Loss Profiles, and Lesion Depth Measurements*

The integrated reflectivity and integrated mineral loss were calculated in each of the six areas on the sample. Line profiles were taken from the orthogonal polarization (⊥-axis) PS-OCT images or b-scans in each of the six regions. The reflectivity was integrated from the dentin surface to a real depth of 300 $\mu$m, yielding the integrated reflectivity $\Delta R$ of the regions in units of (dB·$\mu$m). The real depth was calculated by dividing the optical depth by the refractive index of dentin, 1.5.[26] The lesion depth was estimated by taking the depth at which the intensity dropped to a level equivalent to $1/e^2$, the peak intensity. Previous studies of demineralization on enamel surfaces have shown that $\Delta R$ correlates directly with the integrated mineral loss (vol. % mineral·$\mu$m) called $\Delta Z$.[6] Similarly, line profiles were taken from the digital TMR of the thin sections cut along the same position scanned by OCT. X-ray attenuation was converted to volume percent mineral using a sound enamel calibration curve. The line profiles in the four treatment (lesion) areas were subtracted from the sound mineral profiles to yield the integrated mineral loss. Demineralized lesions will shrink in dry conditions, as is visible in PS-OCT and TMR scans; hence, the line profiles were integrated from an extrapolated edge of the sample to a depth of 300 $\mu$m to give units of $\Delta Z$ (vol. %·$\mu$m). The integrations were performed using Igor Pro software (Wavemetrics, Lake Oswego, Oregon). Prior to taking the line profiles for the OCT images, a $10 \times 10$ convolution filter was applied to reduce speckle in the images. Sample groups were compared using analysis of variance (ANOVA) with a Tukey-Kramer *post-hoc* multiple comparisons test. A paired t-test was used when only two groups were under consideration. Instat™ from (GraphPad Software, San Diego, California) was used for the statistical calculations.

## 3 Results

Reflected light images of one of the dentin samples after exposure to the demineralization and remineralization solutions is shown in Fig. 1. The demineralization window (D) appears whiter or more opaque than the remineralization window ($R$), as would be expected if additional mineral has been deposited in the area exposed to remineralization. PS-OCT scans were acquired along the long axis of each sample near the center and sectioned for PLM and TMR in the same orientation.

Figures 2 and 3 each contain a (⊥-axis) PS-OCT b-scan image [Figs. 2(a) and 3(a)], the corresponding TMR [Figs. 2(b) and 3(b)], and PLM images for thin sections cut from the same sample with a similar orientation [Figs. 2(c) and 3(c)]. A red-white-blue false color scheme is used for the PS-OCT images with the intensity scale in decibel units (dB), where red and white areas have the highest reflectivity. A similar red-white-blue false color scheme was also used for the volume percent mineral content in the TMR images. The reflectivity of sound dentin is relatively high due to its high scattering coefficient. The lower range of the intensity scale for the PS-OCT images was intentionally set to maximize the contrast of the demineralized dentin in Figs. 2 and 3. Therefore, the sound areas appear blue. The demineralization was most severe in the region marked (D) as anticipated, while the areas exposed to the remineralization solution (R) typically had a layer of intact mineral of enhanced mineral content.

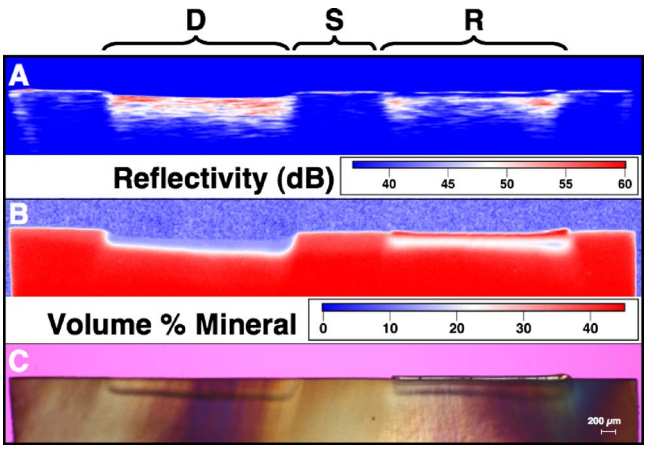


**Fig. 2** (a) (⊥-axis) PS-OCT scan taken along the long axis of a sample before sectioning. Intensity scale is shown in red-white-blue in units of decibels (dB). Remineralized layer is visible as a blue gap above the remineralized lesion. (b) The corresponding transverse microradiograph (TMR) of a 260-$\mu$m-thick section in a similar orientation to the PS-OCT image. The intensity scale is also shown in red-white-blue with units in volume percent mineral. (c) The PLM image of the same section shown at 15× magnification (Color online only).

Dentin contains a high percentage of collagen, and demineralized dentin tends to shrink considerably when exposed to air, i.e., if it is not immersed in water. This can be seen in Figs. 2 and 3. PS-OCT and TMR were carried out with wet samples in air, while for PLM the samples were immersed in

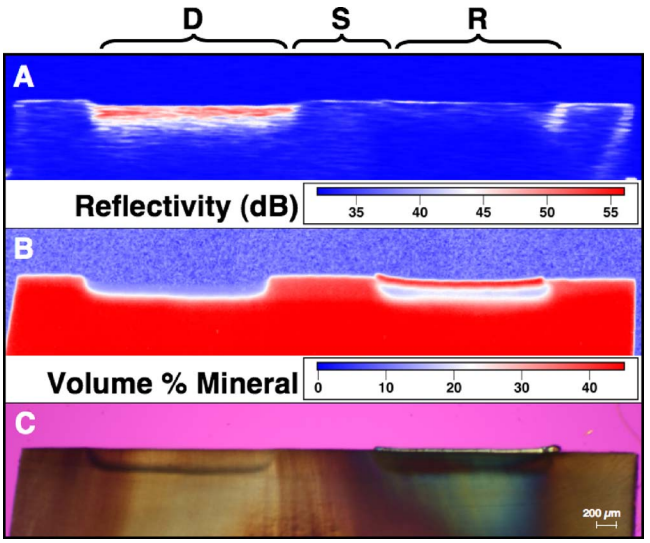


**Fig. 3** (a) (⊥-axis) PS-OCT scan of another sample before sectioning. Remineralized lesion has a significantly lower intensity compared to the demineralization lesion. (b) The corresponding transverse microradiograph (TMR) of a 260-$\mu$m-thick section in a similar orientation to the PS-OCT image. (c) The PLM image of the same section shown at 15× magnification.

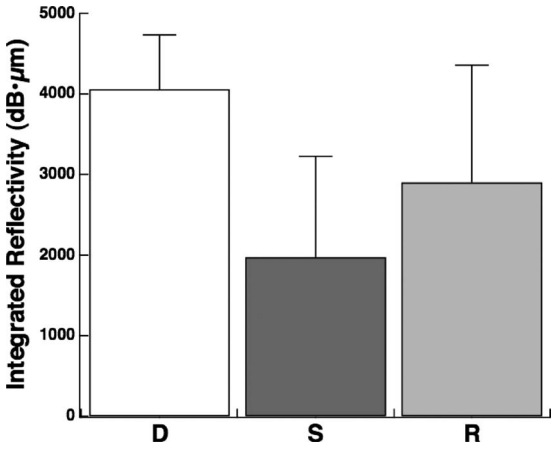


**Fig. 4** Mean±SD values of the integrated reflectivity $\Delta R$ measured with PS-OCT for the three treatment groups D, S, and R (n=15). The integrated reflectivity values were calculated to a depth of 300 $\mu$m.

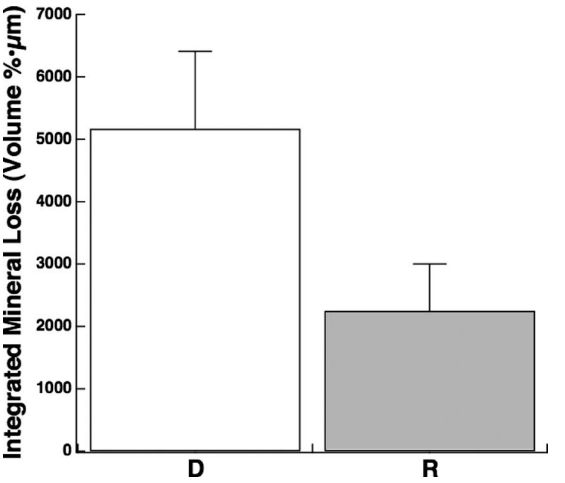


**Fig. 5** Mean±SD values of the integrated mineral loss $\Delta Z$ measured with TMR for the two treatment groups D and R (n=15). The integrated mineral loss values were calculated to a depth of 300 $\mu$m.

water. There is considerable shrinkage in the demineralized regions for the PS-OCT and TMR images, while the PLM images show minimal shrinkage in those regions. It is interesting to note that shrinkage typically did not occur in the remineralized window (R), since the highly mineralized intact surface zone prevented loss of water from the lesion area. The intact surface area was highly transparent when viewed under polarized light microscopy and had a high mineral content, ~60% mineral. This is 10% higher than sound dentin.

Individual a-scans were chosen from the center of each of the two areas on each sample. The mean integrated reflectivity in units of dB•$\mu$m was calculated by integrating the reflectivity in the orthogonal polarization ($\perp$) image in units of decibels (dB) to a depth of 300 $\mu$m. The volume percent mineral loss was measured in the same location for TMR and integrated over the same depth, 300 $\mu$m, to yield the integrated mineral loss in vol. %•$\mu$m. The mean ± SD ($\Delta R$) values for the demineralization (D), sound ($S$), and the remineralization ($R$) groups are displayed in Fig. 4. The lesion depth was also measured with PLM and PS-OCT, and these measurements are tabulated in Table 1 for the remineralization and demineralization groups, respectively.

The dentin shrinkage introduces an error in $\Delta Z$, since the calibration curve used to determine mineral content is not accurate for mineral content below 10%.[25] Hence, shrinkage of the lesions (see Figs. 2 and 3) leads to an overestimation of the mineral loss by TMR. The mean ± SD ($\Delta Z$) values for the demineralization (D), sound (S), and remineralization (R) groups are displayed in Fig. 5.

The lesion depth was also calculated from OCT images and polarized light microscopy, and those values are tabulated in Table 1. The lesion depths in the demineralization (D) and remineralization (R) zones, as well as the estimated thickness of the surface layer of highly increased mineral content in the remineralization zone ($R_L$), agreed quite well between the three methods of PS-OCT, TMR, and PLM, as can be seen in Fig. 6. The mean ± SD of the thickness of the layer of increased mineral content was measured to be 55 ± 12 $\mu$m using TMR, 58 ± 14 $\mu$m using PS-OCT, and 53 ± 15 $\mu$m using PLM. Correlation plots of the lesion depth measured using PS-OCT versus TMR and PLM are shown in Figs. 7 and 8. These indicate that the three methods manifest a reasonably

**Table 1** PS-OCT, PLM, and TMR measurements for all six groups' mean±SD. Groups in the same row with a different letter are significantly different ($p<0.05$) n=15.

| | D | S | R |
|---|---|---|---|
| PS-OCT (dB•$\mu$m) | 4058±672 a | 1978±1250 b | 2901±1460 c |
| TMR (vol. %•$\mu$m) | 5170±1240 a | | 2256±757 b |
| PS-OCT ($\mu$m) | 204±37 a | | 228±34 b |
| PLM ($\mu$m) | 215±31 a | | 240±30 b |
| TMR ($\mu$m) | 163±23 a | | 202±23 b |

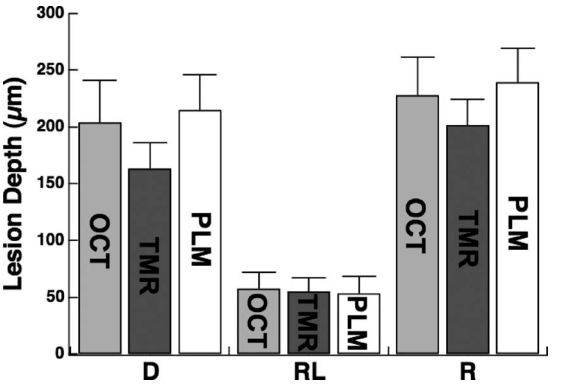


**Fig. 6** Mean±SD values of lesion depth calculated from PS-OCT with light gray bars, TMR with dark gray bars, and PLM images with white bars comparing the three treatment groups of demineralized lesion (D), remineralized layer thickness (RL), and the entire lesion depth after exposure to remineralization (R) (n=15).

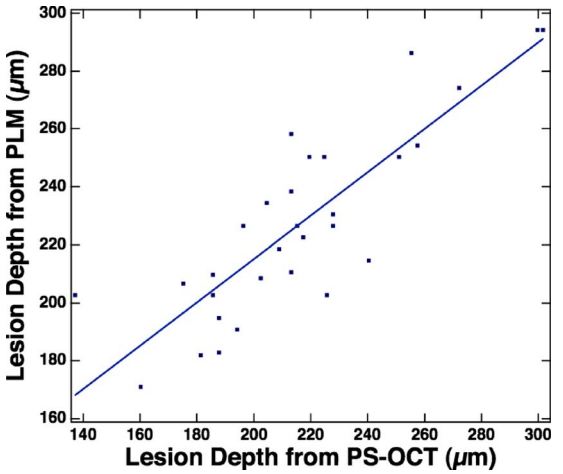


**Fig. 7** Plot of calculated lesion depth from PLM versus PS-OCT images for the D and R study groups (n=30) with the corresponding regression line ($P_r$=0.85).

high correlation. Depths from areas of both demineralization and remineralization are combined in the correlation plots.

## 4 Discussion

The reflectivity from the artificial lesion areas exposed only to the demineralization solution were significantly higher than the lesion areas exposed to the same demineralization solution followed by subsequent exposure to a remineralization solution for 20 days. This demonstrates that PS-OCT can successfully be used to measure the deposition of new mineral in lesion areas, particularly near the surface. In many of the lesion areas exposed to remineralization, there was a highly transparent zone (PLM) of high mineral content that was deposited on the surface of the lesion. The mineral content of that outer zone was more than 60% mineral by volume, which is greater than sound dentin. The high transparency and mineral density of this zone suggests the growth of a highly oriented crystalline phase of apatite. A simple precipitation of calcium phosphate or hydroxyapatite on the surface would produce a rough and opaque white polycrystalline deposit. We have observed both transparent and opaque surface layers formed on the surface of enamel after exposure to a similar regimen of remineralization.[9] PLM images show that the layer of higher mineral content extends above the original dentin surface, which may suggest that the layer may be a precipitate on the lesion surface. However, the surface layer had sufficient mechanical integrity to remain intact during the sectioning process, which indicates that the newly deposited mineral layer is well integrated into the underlying dentin. It is interesting to note that the zone of remineralization is thicker and more pronounced on dentin compared to enamel based on previous imaging studies.[8] Moreover, a definitive zone of remineralization was present on virtually all the dentin samples, while the formation of the outer remineralization layer was less consistent on enamel.

One can postulate that the presence of the outer zone of high mineral content indicates that the active lesion has become arrested, and that further chemical intervention is not necessary. If this is validated clinically, then PS-OCT imaging would present a valuable nondestructive method for assessing nonsurgical intervention.

The excellent agreement among the respective lesion depths and the thickness of the zone of remineralization measured using PLM, TMR, and PS-OCT further demonstrates the diagnostic potential of PS-OCT for root caries lesions.

In conclusion, this study demonstrates that PS-OCT can be used to measure remineralization on dentin surfaces and detect the formation of a zone of highly mineralized dentin on the lesion surface after exposure to a remineralization solution. Further work is needed to demonstrate that PS-OCT can be used to measure the remineralization of natural caries lesions both *in vitro* and *in vivo*.

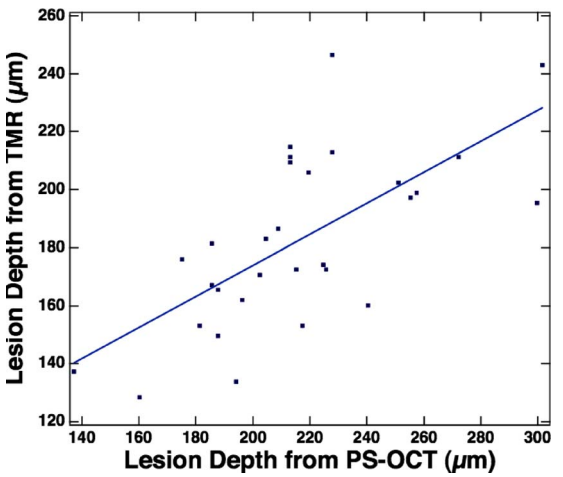


**Fig. 8** Plot of calculated lesion depth from TMR versus PS-OCT images for the D and R study groups (n=30) with the corresponding regression line ($P_r$=0.67).

### *Acknowledgments*

The authors acknowledge the support of NIH grants R01-DE017869 and R01-DE14698 and the help of Dennis Hsu and Chulsung Lee.

### *References*

1. D. Huang, E. A. Swanson, C. P. Lin, J. S. Schuman, W. G. Stinson, W. Chang, M. R. Hee, T. Flotte, K. Gregory, C. A. Puliafito et al., "Optical coherence tomography," *Science* **254**, 1178–1181 (1991).
2. B. E. Bouma, G. J. Tearney, Eds., *Handbook of Optical Coherence Tomography*, Marcel Dekker, New York (2002).
3. M. Brezinski, *Optical Coherence Tomography: Principles and Applications*, Elsevier, London (2006).
4. M. R. Hee, D. Huang, E. A. Swanson, and J. G. Fujimoto, "Polarization-sensitive low-coherence reflectometer for birefringence characterization and imaging," *J. Opt. Soc. Am. B* **9**, 903–908 (1992).
5. S. L. Chong, C. L. Darling, and D. Fried, "Nondestructive measurement of the inhibition of demineralization on smooth surfaces using polarization-sensitive optical coherence tomography," *Lasers Surg. Med.* **39**(5), 422–427 (2007).
6. S. K. Manesh, C. L. Darling, and D. Fried, "Nondestructive assessment of dentin demineralization using polarization sensitive optical coherence tomography," *J. Biomed. Mater. Res.* (in press).
7. C. Lee, C. Darling, and D. Fried, "Polarization, sensitive optical coherence tomographic imaging of artificial demineralization on exposed surfaces of tooth roots," *Dent. Mater.* **25**(6), 721–728 (2009).
8. A. M. Can, C. L. Darling, and D. Fried, "High-resolution PS-OCT of enamel remineralization," *Proc. SPIE* **6843**, 68430T-7 (2008).
9. R. S. Jones, C. L. Darling, J. D. B. Featherstone, and D. Fried, "Remineralization of in vitro dental caries assessed with polarization sen-

sitive optical coherence tomography," *J. Biomed. Opt.* **11**(1), 014016 1–9 (2006).
10. R. S. Jones, and D. Fried, "Remineralization of enamel caries can decrease optical reflectivity," *J. Dent. Res.* **85**(9), 804–808 (2006).
11. R. S. Jones, M. Staninec, and D. Fried, "Imaging artificial caries under composite sealants and restorations," *J. Biomed. Opt.* **9**(6), 1297–1304 (2004).
12. R. S. Jones, C. L. Darling, J. D. B. Featherstone, and D. Fried, "Imaging artificial caries on occlusal surfaces with polarization sensitive optical coherence tomography," *Caries Res.* **40**(2), 81–89 (2004).
13. R. S. Jones, and D. Fried, "The effect of high index liquids on PS-OCT imaging of dental caries," *Proc. SPIE* **5687**, 34–41 (2005).
14. P. Ngaotheppitak, C. L. Darling, and D. Fried, "Polarization optical coherence tomography for the measuring the severity of caries lesions," *Lasers Surg. Med.* **37**(1), 78–88 (2005).
15. D. Fried, J. Xie, S. Shafi, J. D. B. Featherstone, T. Breunig, and C. Q. Lee, "Early detection of dental caries and lesion progression with polarization sensitive optical coherence tomography," *J. Biomed. Opt.* **7**(4), 618–627 (2002).
16. H. Shemesh, G. van Soest, M. K. Wu, L. W. van der Sluis, and P. R. Wesselink, "The ability of optical coherence tomography to characterize the root canal walls," *J. Endod.* **33**(11), 1369–1373 (2007).
17. H. Shemesh, G. van Soest, M. K. Wu, and P. R. Wesselink, "Diagnosis of vertical root fractures with optical coherence tomography," *J. Endod.* **34**(6), 739–742 (2008).
18. D. Fried, J. D. B. Featherstone, R. E. Glena, and W. Seka, "The nature of light scattering in dental enamel and dentin at visible and near-IR wavelengths," *Appl. Opt.* **34**(7), 1278–1285 (1995).
19. C. L. Darling, G. D. Huynh, and D. Fried, "Light scattering properties of natural and artificially demineralized dental enamel at 1310-nm," *J. Biomed. Opt.* **11**(3), 034023 (2006).
20. B. T. Amaechi, A. Podoleanu, G. Komarov, S. M. Higham, and D. A. Jackson, "Optical coherence tomography for dental caries detection and analysis," *Proc. SPIE* **4610**, 100–108 (2002).
21. D. Fried, J. Xie, S. Shafi, J. Featherstone, T. M. Breunig, and C. Q. Le, "Imaging caries lesions and lesion progression with polarization optical coherence tomography," *Proc. SPIE* **4610**, 113–124 (2002).
22. *Dental Caries: The Disease and Its Clinical Management*, O. Fejerskov, and E. Kidd, eds, Blackwell, Oxford (2003).
23. J. D. B. Featherstone, N. A. Barrett, M. G. Conners, and M. Shariati, "A pH cycling model for assessing fluoride effects on root caries," *J. Dent. Res.* **68**, 995 (1989).
24. J. Bush, P. Davis, and M. A. Marcus, "All-fiber optic coherence domain interferometric techniques," *Proc. SPIE* **4204**, 71–80 (2000).
25. C. L. Darling, J. D. B. Featherstone, C. Q. Le, and D. Fried, "An automated digital microradiography system for assessing tooth demineralization," *Proc. SPIE* **7162**, 1–7 (2009).
26. X. J. Wang, T. E. Milner, J. F. de Boer, Y. Zhang, D. H. Pashley, and J. S. Nelson, "Characterization of dentin and enamel by use of optical coherence tomography," *Appl. Opt.* **38**(10), 2092–2096 (1999).